0026-895X/93/020302-11$03.00/0

MOLECULAR PHARMACOLOGY, 43:302-312

Pharmacological Characterization of a Receptor for Platelet-Activating Factor on Guinea Pig Peritoneal Macrophages using [^{3}H]Apafant, a Selective and Competitive Platelet-Activating Factor Antagonist: Evidence that the Noncompetitive Behavior of Apafant in Functional Studies Relates to Slow Kinetics of Dissociation

PATRICK C. RING, PAUL M. SELDON, PETER J. BARNES, and MARK A. GIEMBYCZ
Department of Thoracic Medicine, Royal Brompton National Heart and Lung Institute, London SW3 6LY, United Kingdom
Received May 22, 1992; Accepted October 19, 1992

SUMMARY

In this paper we report the characterization of a receptor for platelet-activating factor (PAF) on guinea pig peritoneal macrophages, using a radiolabeled hydrophilic PAF antagonist, [^{3}H] apafant. [^{3}H]Apafant bound to intact macrophages in a concentration-dependent manner that was specific, saturable, reversible, and inhibited competitively by C_{16}-PAF (1-*O*-octadecyl-2-*O*-acetyl-*sn*-glyceryl-3-phosphocholine). Scatchard transformation and Hill analysis of these data revealed that [^{3}H]apafant identified a homogeneous population of noninteracting sites with a pK_d of 8.22 nM and a B_{max} of 31,600 sites/cell. The rate at which [^{3}H] apafant associated with ($K_{on} = 2.9 \times 10^6$ M$^{-1}\cdot$min^{-1}) and dissociated from ($K_{off} = 0.043$ min^{-1}) intact macrophages was slow, with $t_{1/2}$ values of 15 and 50 min, respectively; the kinetically derived pK_d was 8.3. In competition studies C_{16}-PAF inhibited in a biphasic manner the binding of [^{3}H]apafant to intact macrophages, which could be resolved into high ($pK_i = 8.27$; 60%) and low ($pK_i = 6.06$; 40%) affinity components. In macrophage membranes, the affinity of C_{16}-PAF ($pK_i = 8.48$) determined from competition studies with [^{3}H]apafant was significantly reduced ($pK_i = 6.95$) by guanosine-5′-*O*-(3-thio)triphosphate, whereas the mean slope of the inhibition curves was increased from 0.470 to 0.700. Functionally, C_{16}-PAF (10 nM to 10 μM) evoked concentration-dependent $\cdot O_2^-$ generation that was biphasic in nature. Pretreatment of macrophages with apafant antagonized in a noncompetitive manner the first phase of C_{16}-PAF (<100 nM)-induced respiratory burst, whereas the second component (>1 μM C_{16}-PAF) of this response was unaffected. It is concluded that guinea pig peritoneal macrophages express receptors for PAF for which apafant has high affinity. The biphasic competition curves obtained with C_{16}-PAF in binding experiments and the effect of guanosine-5′-*O*-(3-thio)triphosphate are consistent with the hypothesis that these apafant-sensitive PAF receptors are coupled to guanine nucleotide-binding proteins and can exist in at least two guanine nucleotide-regulated conformational states. It is also suggested that the noncompetitive antagonism of PAF-induced $\cdot O_2^-$ generation by apafant may be a consequence of the slow rate at which this antagonist dissociates from PAF receptors on intact macrophages.

PAF is a potent, biologically active, ether-linked phospholipid composed of several structurally related homologues, of which 1-*O*-hexadecyl- and 1-*O*-octadecyl-2-*O*-acetyl-*sn*-glyceryl-3-phosphocholine are the predominant naturally occurring species (1, 2). These lipids exert diverse physiological and pharmacological actions *in vivo* and *in vitro* and, moreover, have been implicated in the pathogenesis of many disorders, in particular inflammation, airways hyperreactivity, bronchial asthma, anaphylaxis, and a variety of acute allergic reactions (3).

The cell types upon which PAF acts to promote the aforementioned pathologies are at present uncertain. However, with respect to inflammation recent evidence suggests that one target may be macrophages, which are found in large numbers at inflammatory loci. Support for this contention derives from reports that have documented that alveolar and peritoneal macrophages from a number of species exhibit a range of biochemical and functional responses to PAF that are generally proinflammatory in nature. These include the elaboration of highly reactive oxygen-derived free radicals (4–7) and the generation of other proinflammatory mediators derived from arachidonic acid (8–11). In addition, PAF is chemotactic for macrophages (12), enhances glucose utilization by these cells (13), and promotes polyphosphoinositide hydrolysis (5, 12) with attendant Ca^{2+} mobilization (12, 14).

In many cell types the actions of PAF are believed to be mediated by specific cell surface receptors (see Refs. 15 and 16). Indeed, Shimizu and colleagues (17, 18) have recently

The authors acknowledge the Medical Research Council (UK) for financial support.

ABBREVIATIONS: PAF, platelet-activating factor; apafant (WEB 2086), 3-[4-(chlorophenyl)-9-methyl-*H*-thienol[3,2-*f*][1,2,4]triazolo[4,3-*a*][1,4]diazepin-2-yl]-(4-morpholinyl)-1-propanone; bepafant (WEB 2170), 6-(2-chlorophenyl)-8,9-dihydro-1-methyl-8-(4-morpholinylcarbonyl)-4*H*,7*H*-cyclopenta[4,5]thieno[3,2-*f*][1,2,4]triazolo[4,3-*a*]diazepine; STY 2108, 6-(2-chlorophenyl)-8,9-dihydro-1-methyl-8-(*N*-morpholinomethyl)-4*H*,7*H*-cyclopenta[4,5]thieno[3,2-*f*]triazolo[4,3-*a*][1,4]diazepine; UK 74,505, 4-(2-chlorophenyl)-6-methyl-2-[4-(2-methylimidazol[4,5-*c*]pyrid-1-yl)phenyl]-5-(2-pyridylcarbamoyl)-1,4-dihydropyridine-3-carboxylic acid ethyl ester; BN 50739, tetrahydro-4,8,9,10-methyl-(chloro-2-phenyl)-6-[(dimethoxy-3,4-phenyl)thio]methylthiocarbonyl-9-pyrido[4′,3′-4,5]thieno[3,2-*f*]triazolo-1,2,4[4,3-*a*][1,4]diazepine; BN 50741, 6-(2-chlorophenyl)-9-[[4-(1,1-dimethylethyl)phenyl]sulfonyl]-7,8,9,10-tetrahydro-1-methyl-4*H*-pyrido[4′,3′-4,5]thieno[3,2-*f*][1′,2′,4]triazolo[4,3-*a*][1,4]diazepine; GDPβS, guanosine-5′-*O*-(2-thio)diphosphate; GTPγS, guanosine-5′-*O*-(3-thio)triphosphate; BSA, bovine serum albumin; PIPES, piperazine-*N*,*N*′-bis[2-ethanesulfonic acid]; HBSS, Hanks' balanced salt solution; HEPES, 4-(2-hydroxyethyl)-1-piperazineethanesulfonic acid; TLC, thin layer chromatography; OAGPC, 1-*O*-octadecyl-2-*O*-arachidonoyl-*sn*-glyceryl-3-phosphocholine; DMSO, dimethylsulfoxide; $\cdot O_2^-$, superoxide anion C_{18}-PAF, 1-*O*-octadecyl-2-*O*-acetyl-*sn*-glyceryl-3-phosphocholine; *lyso*-C_{18}-PAF, 1-*O*-octadecyl-2-*lyso*-*sn*-glyceryl-3-phosphocyline.

reported the cloning and expression of a PAF receptor from guinea pig lung parenchyma and human leukocytes. On platelets, neutrophils, and eosinophils, specific binding sites for PAF have been identified that have the characteristics of *bona fide* receptors (15). Although previous studies have provided some evidence that the actions of PAF on macrophages also are receptor mediated (6, 19, 20), these PAF receptors have not been definitively characterized. This is almost certainly due to the fact that, until relatively recently, the only radioligand available commercially with which to study PAF receptors was the natural agonist [^{3}H]PAF. It is well documented that the use of agonists to label receptors in binding studies has certain drawbacks. With respect to PAF these are manifold. Thus, not only does PAF activate target cells but also it is likely to be rapidly metabolized. Moreover, PAF is a very lipophilic molecule, a property that promotes high levels of nonspecific binding, specific non-receptor binding, and the labeling of internalized and/or intracellular receptors (15). Collectively, therefore, these limitations effectively preclude the routine use of [^{3}H] PAF to determine cell surface receptor number and ligand affinity.

More recently a number of hydrophilic PAF antagonists have been developed that are now available in radiolabeled form at a specific activity sufficient for use in binding experiments (15, 21, 22). The principal objective of this study, therefore, was to utilize [^{3}H]apafant, a new, cell-impermeant, PAF antagonist, 1) to identify and characterize the cell surface PAF receptors expressed by guinea pig peritoneal macrophages and 2) to evaluate its potential for use in radioligand binding studies.

A preliminary account of some of these data has been presented to the British Pharmacological Society (23) and to the British Association for Lung Research (24).

Materials and Methods

Induction, harvesting, and purification of macrophages. Macrophages were elicited in the peritoneum of male Dunkin-Hartley guinea pigs (600–1400 g) by weekly intraperitoneal injection of human serum (1 ml/animal), obtained as a byproduct of human granulocyte isolations. This procedure led to the production of eosinophil/macrophage-rich peritoneal exudates, substantially or entirely devoid of neutrophils and platelets, within 2–6 weeks.

Three to 6 days after plasma injection guinea pigs were anesthetized with ketamine (25 mg/kg of body weight) and xylazine (5 mg/kg) and the peritoneal cavity of each animal was lavaged with 50 ml of sterile 5% (w/v) glucose injected via a 17-gauge cannula. The lavage fluid was aspirated into conical polypropylene centrifugation tubes and centrifuged at 240 × *g* for 10 min at 4° to pellet cells. These were then washed in HBSS, pooled, and finally resuspended in Percoll (1.070 g/ml)-containing buffer A (25 mM PIPES, pH 7.4, 110 mM NaCl, 5 mM KCl, 5.4 mM glucose) supplemented with 20% (v/v) fetal calf serum and 30 μg/ml DNase.

Macrophages were separated from other cell types by centrifugation of the pooled cell preparation at 1600 × *g* for 20 min at 18° over discontinuous Percoll gradients (1.070, 1.080, 1.085, 1.090, and 1.100 g/ml in buffer A), according to the method of Gartner (25). Using this procedure macrophages were recovered from the 1.070/1.080 g/ml Percoll interface and were >95% pure and >96% viable, as assessed by trypan blue exclusion. Macrophages either were used immediately for binding or functional studies or were pelleted and frozen at −20° for subsequent membrane preparation.

Preparation of macrophage membranes. Frozen macrophages (~1 × 10^8 cells/ml) were subjected to osmotic lysis in ice-cold buffer B (10 mM Tris·HCl, pH 7.0, 10 μM phenylmethylsulfonyl fluoride), followed by rapid freezing in liquid nitrogen and slow thawing at room temperature. The cell lysate was sonicated (MSE Soniprep 150 with probe attachment) for 10 sec at full power and then centrifuged at 27,000 × *g* for 20 min at 4°. The resulting membrane pellet was washed once in buffer B and finally resuspended at a protein concentration of ~1 mg/ml in buffer B supplemented with a proteinase inhibitor mixture consisting of 10 μM leupeptin, 10 μM pepstatin A, and 20 μg/ml soybean trypsin inhibitor. Membranes were stored at −80° until required. Protein was solubilized from the membranes with 1 M NaOH and was subsequently quantified according to the method of Lowry *et al.* (26), using BSA as standard.

Radioligand binding studies. Guinea pig intact macrophages (0.5–8 × 10^6 cells) or macrophage membranes (50–200 μg of protein) were incubated in duplicate at 25° in buffer C (10 mM HEPES, pH 7.4, 145 mM NaCl, 4.8 mM KCl, 1.6 mM $MgCl_2 \cdot 6H_20$, 6 mM glucose, 0.6 mM NaH_2PO_4, 0.4 mM K_2HPO_4, 0.1%, w/v, BSA) containing [^{3}H] apafant (1–200 nM), in a final volume of 500 μl. In some experiments the ability of C_{18}-PAF, *lyso*-C_{18}-PAF, and a number of structurally dissimilar PAF antagonists to compete with [^{3}H]apafant for binding to intact macrophages was evaluated. Binding reactions were terminated at the desired times (see "Results" for details) by rapid filtration through Whatman GF/C glass fiber filters that had been presoaked for 60 min in buffer C containing 1% (w/v) BSA and that were then washed with 2 × 4 ml of ice-cold buffer C. The radioactivity retained by each filter was measured by liquid scintillation counting in 4 ml of Filtron X (National Diagnostics, Hemel Hempstead, UK), at a counting efficiency of approximately 60%. Specific binding was determined experimentally from the difference between [^{3}H]apafant bound in the absence and presence of a large molar excess (10 μM) of unlabeled apafant. Preliminary studies revealed that the specfic binding of [^{3}H] apafant was proportional to macrophage number (up to 8 × 10^6 cells/incubate) and membrane protein (up to 200 μg/incubate).

Data analysis. Data were analyzed by nonlinear least-squares iterative curve-fitting using the Inplot computer program (GraphPad Inc., San Diego, CA). Saturation binding isotherms were analyzed assuming that data conformed to either a single or double hyperbola, and the goodness of fit was evaluated by measuring the residual sum of the squares (an index of the variability between the fitted and experimentally determined data). Values for K_d and B_{max} were subsequently determined from Scatchard transformation of these data. Re-

sults derived from competition studies were analyzed for one or two sites and the goodness of fit was assessed as described above. All IC_{50} values derived from competition experiments were converted to K_i values, using the Cheng and Prusoff (27) correction, to facilitate comparison with values for other ligands reported in the literature. In kinetic studies the association of [^{3}H]apafant was considered to be pseudo-first-order because the concentration (10 nM) of radioligand bound to both intact cells and membranes at equilibrium did not exceed 5% of the total amount of radiolabel used. The association rate constant (k_{on}) was thus calculated from the observed association rate constant (k_{obs}), determined experimentally, using the equation $k_{on} = (k_{obs} - k_{off})/[L]$, where k_{off} is the dissociation rate constant and $[L]$ is the concentration of [^{3}H]apafant used (10 nM). Because the dissociation of [^{3}H]apafant depends only upon the initial concentration of [^{3}H]apafant-receptor complex at equilibrium, the kinetics of this process are first-order. The k_{off} was thus derived from the slope of the first-order plot of the logarithmically transformed data describing the displacement of [^{3}H]apafant (10 nM), bound at equilibrium, by a large molar excess (10 μM) of unlabeled apafant. The kinetically derived K_d was subsequently calculated from the expression $K_d = k_{off}/k_{on}$.

Metabolism of C_{18}-PAF. Guinea pig intact peritoneal macrophages (~4 × 10^6) were suspended in buffer C containing 0.4 pmol of [^{3}H]C_{18}-PAF (~1.6 × 10^5 dpm/pmol) in the absence and presence of 5 μM unlabeled C_{18}-PAF, in a total volume of 500 μl, and were incubated at 25°. Control incubations without cells and unlabeled C_{18}-PAF were run in parallel to assess the magnitude of nonenzymatic degradation. Incubations were terminated after 1, 2, and 3 hr by the addition of 1.5 ml of chloroform/methanol (1:1), vortex mixed, and centrifuged at 3000 × *g* for 10 min to separate phases. The upper aqueous phase was removed by aspiration and 400 μl of the remaining solvent phase containing lipids were dried under nitrogen gas. The extracted lipids were resuspended in methanol (50 μl) and spotted onto 19-lane LK6DF TLC silica gel 60A plates (Whatman, Maidstone, Kent, UK), which were subsequently developed in an acidic solvent system consisting of chloroform/methanol/acetic acid/distilled water (75:50:10:6, v/v). Reference lipids ([^{3}H]C_{18}-PAF, C_{18}-PAF, *lyso*-C_{18}-PAF, and OAGPC) were dissolved in methanol and subjected to TLC in the same way. When the solvent front had reached the top of the plate (running time, ~90 min at 22°) the chromatogram was allowed to dry and was sprayed lightly with 2′,7′-dichlorofluorescene and the lipids were visualized under UV light at 270 nm. The extent of C_{18}-PAF metabolism and chromatographic identity of the primary metabolites of C_{18}-PAF were then quantified by liquid scintillation counting, by scraping each lane of the TLC plate in 5-mm strips and counting them in 2 ml of Filtron X. The R_F values of the lipid standards chromatographed under the aforementioned conditions were as follows: [^{3}H]C_{18}-PAF/C_{18}-PAF, 0.43; *lyso*-C_{18}-PAF, 0.19; and OAGPC, 0.68.

Measurement of respiratory burst. The generation of $\cdot O_2^-$ by guinea pig peritoneal macrophages was used as an index of respiratory burst activity and was determined by measuring the superoxide dismutase (37.5 units/ml)-inhibitable reduction of ferricytochrome *c* (28), essentially as described by Pick and Mizel (29). Assays were perfomed at 37° in 96-well microtiter plates and were initiated by the addition of 20 μl of C_{18}-PAF (1 pM to 10 μM) to 180 μl of HBSS containing ferricytochrome *c* (100 μM) and macrophages (~1 × 10^5 cells) that had been preincubated for 5 min with apafant (10 nM to 100 μM) or its ethanol/water vehicle. Microtiter plates were vortex mixed and maintained at 37° for 30 min in a thermostatically controlled incubator. Changes in absorbance were then measured spectrophotometrically at 550 nm in a Dynatech MR 700 microtiter plate reader. Superoxide anion generation was calculated from the molar extinction coefficient of ferricytochrome *c* (21.1 × 10^3 cm^2/mol), making appropriate correction for the fact that the vertical path length in each well was 5.6 mm when 200-μl reaction volumes were used. Data are expressed in the text and relevant figure legends as nmol of ferricytochrome *c* reduced in 30 min per 1 × 10^6 cells.

Drugs and analytical reagents. The following drugs and analytical reagents were obtained from the Sigma Chemical Co. (Poole, Dorset, UK): C_{18}-PAF, *lyso*-C_{18}-PAF, GDPβS, GTPγS, DMSO, ferricytochrome *c* (type III), superoxide dismutase (from bovine erythrocytes), 2′,7′-dichlorofluorescene, and BSA. All other reagents were obtained from the following sources: HBSS, Flow Laboratories Ltd. (Rickmansworth, Surrey, UK); OAGPC, Cascade Biochem Ltd. (Reading, Berkshire, UK); Percoll, Pharmacia (Uppsala, Sweden); apafant, bepafant, and STY 2108, Boehringer Ingelheim KG (Ingelheim am Rhein, Germany); BN 50739 and BN 50741, Institute Henri Beaufour (Paris, France); UK 74,505, Pfizer Central Research (Sandwich, Kent, UK); [^{3}H]apafant (~17 Ci/mmol), New England Nuclear (Boston, MA); and 1-*O*-[^{3}H]octadecyl-2-*O*-acetyl-*sn*-glyceryl-3-phosphocholine (92 Ci/mmol), Amersham International (Buckinghamshire, UK). Unless otherwise stated all other reagents and solvents were obtained from BDH (Poole, Dorset, UK).

Dissolution and storage of drugs. Stock solutions (100 mM) of PAF antagonists were prepared in DMSO (BN 50739 and BN 50741) or absolute alcohol (apafant, bepafant, STY 2108, and UK 74,505) before being diluted to the desired working concentration in aqueous media. C_{18}-PAF, *lyso*-C_{18}-PAF, GTPγS, and GDPβS were dissolved at stock concentrations of 1 mM in the appropriate assay buffer supplemented with 0.1% BSA and were stored at −80° until required. Superoxide dismutase was made up as a stock solution of 300 μg/ml in DMSO and was stored at −80°. All other reagents were dissolved in aqueous media.

Statistical analysis. Data in the text and figure legends refer to the mean ± standard error of *n* independent determinations taken from different cell preparations. Where appropriate, Student's *t* test (two-tailed) or one-way analysis of variance/Newman-Keuls test was used to assess significance between control and treatment groups. The null hypothesis was rejected when $p < 0.05$.

Results

Binding Studies in Intact Macrophages

Equilibrium binding studies. Fig. 1a shows a representative saturation isotherm of the binding of [^{3}H]apafant (1–200 nM) to guinea pig intact peritoneal macrophages. The binding of this radiolabeled antagonist was concentration-dependent, saturable and conformed to a single hyperbola. Nonspecific binding increased linearly as a function of radioligand concentration but was low, amounting to <10% of the total binding at the K_d (Fig. 1a). Scatchard transformation of the specific binding data yielded a linear plot, indicating that [^{3}H]apafant identified a homogeneous population of binding sites (Fig. 1b). In 11 independent experiments the mean equilibrium pK_d of [^{3}H]apafant was 8.25 ± 0.05, with a B_{max} of 52.5 ± 4.7 fmol/10^6 cells. Given that [^{3}H]apafant interacts in a simple competitive manner with guinea pig macrophages (see below), this B_{max} equates to 31,600 ± 2,800 (n = 11) specific binding sites for [^{3}H]apafant per cell.

To determine the nature and stoichiometry of [^{3}H]apafant binding to these cells, Hill plots of the saturation binding isotherms were constructed (Fig. 1b, *inset*). The mean Hill coefficient (n_H) derived from this analysis was 1.04 ± 0.05 (n = 11), which was not significantly different from unity. Consistent with a competitive interaction between these two ligands, inclusion of C_{18}-PAF (10 nM) in the binding cocktail reduced the affinity of [^{3}H]apafant ~2-fold without significantly affecting the B_{max} (control: pK_d = 8.32 ± 0.13, B_{max} = 32,500 ± 3,800, n = 3; +C_{18}-PAF: pK_d = 7.96 ± 0.09, B_{max} = 29,600 ± 3,400, n = 3).

Kinetics of [^{3}H]apafant association and dissociation. At 25° [^{3}H]apafant (10 nM) bound to intact guinea pig perito-

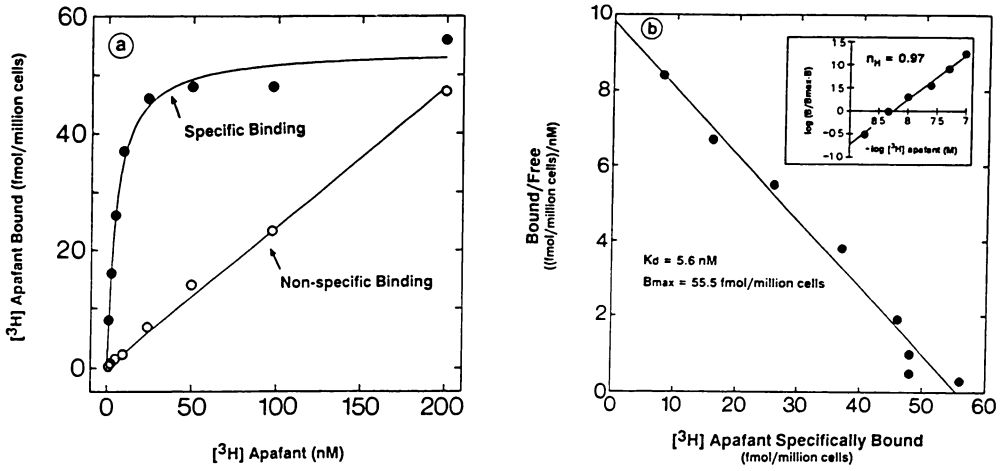

Fig. 1. Binding of [^{3}H]apafant to guinea pig intact peritoneal macrophages. *a*, Representative saturation isotherm for [^{3}H]apafant. Binding was measured at 25° over a concentration range of 1–200 nM in buffer C containing ~3 × 10^6 macrophages/incubate. Nonspecific binding was defined with 10 μM unlabeled apafant. *b*, Scatchard transformation of the data in *a* and the K_d and B_{max} values derived from this experiment. *b*, *inset*, Hill plot of the binding of [^{3}H]apafant to intact macrophages. Results are typical of 11 determinations. See Materials and Methods for further details.

neal macrophages in a time-dependent manner, with a $t_{½}$ of 14.6 ± 0.8 min (n = 3); steady state binding was achieved within 90 min (Fig. 2a). Given that the association of [^{3}H]apafant with intact macrophages is pseudo-first-order (see Materials and Methods), the k_{obs} was 0.043 ± 0.005 $M^{-1} \cdot min^{-1}$ (n = 3) (Fig. 2b).

The dissociation of [^{3}H]apafant (10 nM), specifically bound to macrophages at equilibrium, by a large molar excess (10 μM) of the unlabeled ligand was slow ($t_{½}$ = 49.6 ± 6.6 min, n = 3) and still incomplete after 3 hr (Fig. 3a). Despite these slow kinetics, dissociation was monoexponential, from which a mean k_{off} of 0.014 ± 0.002 min^{-1} (n = 3) was derived (Fig. 3b). From the k_{obs}, k_{off}, and concentration of [^{3}H]apafant used, the kinetically derived pK_d was 8.3.

The slow rate at which [^{3}H]apafant dissociated from intact macrophages in the presence of a large molar excess of unlabeled apafant was also observed when a naturally occurring agonist, C_{18}-PAF (5 μM), was used as the displacing ligand ($t_{½}$ = 40.7 ± 4.5 min, n = 3) (Fig. 4a). In these experiments approximately 20% of [^{3}H]apafant was still specifically bound to the cells after a 3-hr incubation at 25° (Fig. 4a). Moreover, the logarithmically transformed data of this dissociation curve deviated significantly from linearity at late time points (Fig. 4b), which may be related to enzymatic metabolism of C_{18}-PAF by the macrophages (see below).

Competition studies. The ability of C_{18}-PAF and *lyso*-C_{18}-PAF, together with a limited number of structurally dissimilar PAF antagonists, to compete with [^{3}H]apafant for binding to guinea pig intact peritoneal macrophages was determined. With the exception of C_{18}-PAF, which yielded shallow competition curves that could be resolved into high and low affinity components (Fig. 5; Table 1), and *lyso*-C_{18}-PAF, which was inactive, all of the drugs inhibited [^{3}H]apafant binding with slopes not significantly different from unity (Table 2).

Binding Studies in Macrophage Membranes

Equilibrium binding studies. Fig. 6a shows a representative saturation isotherm for the binding of [^{3}H]apafant (1–200 nM) to guinea pig peritoneal macrophage membranes. The binding of this radioligand was concentration-dependent, saturable and conformed to a single hyperbola. Nonspecific binding increased linearly as a function of radioligand concentration, amounting to <15% at the K_d (Fig. 6a). Consistent with the data obtained with intact cells, Scatchard transformation of the specific binding data yielded a linear plot, from which a pK_d of 8.16 ± 0.08 (n = 3) and a B_{max} of 543.3 ± 118 fmol/mg of protein (n = 3) were derived (Fig. 6b). The mean Hill coefficient for the binding off [^{3}H]apafant to three different membranes preparations was 0.92 ± 0.1, which was not significantly different from unity (Fig. 6b, *inset*).

Kinetics of [^{3}H]apafant association and dissociation. At 25° [^{3}H]apafant (10 nM) bound to macrophage membranes in a time-dependent manner, with a $t_{½}$ (8.22 ± 1.1 min, n = 3) and k_{obs} (0.080 ± 0.008 $M^{-1} \cdot min^{-1}$, n = 3) significantly different ($p < 0.01$) from the equivalent kinetic constants obtained for

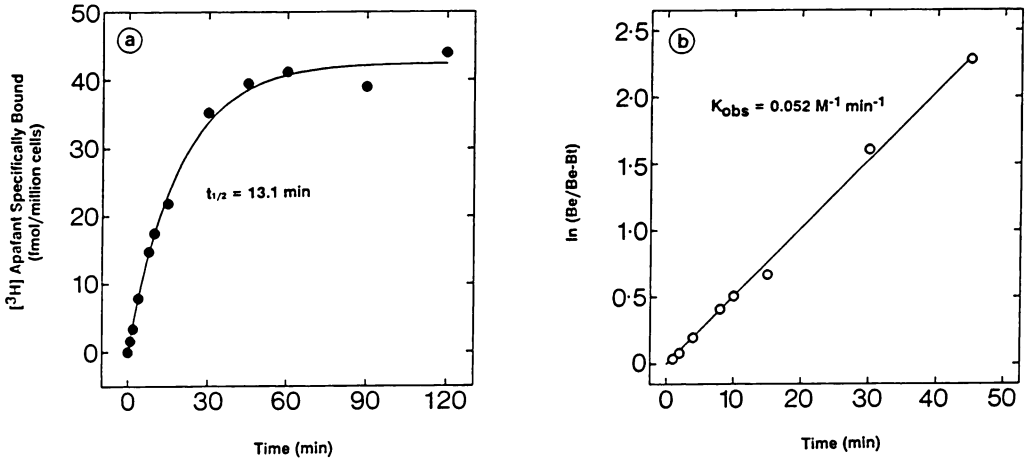

Fig. 2. Association of [^{3}H]apafant with guinea pig intact peritoneal macrophages. [^{3}H]Apafant (10 nM) was incubated at 25° with macrophages (~3 × 10^6/incubate) in buffer C for 1–120 min. Nonspecific binding was defined with 10 μM unlabeled apafant. *a* and *b*, Time course of [^{3}H]apafant association with macrophages and the pseudo-first-order transformation of these data, respectively. Data points represent the mean of duplicate determinations from a single experiment typical of three. See Materials and Methods for further details.

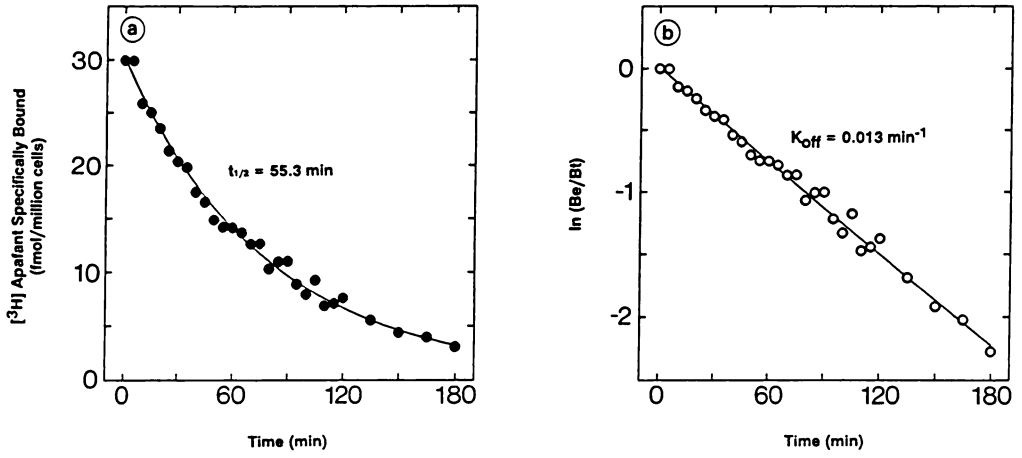

Fig. 3. Dissociation of [^{3}H]apafant from guinea pig intact peritoneal macrophages by unlabeled apafant. [^{3}H]Apafant was incubated with macrophages (~3 × 10^6/incubate) in buffer C for 90 min to achieve steady state binding. Unlabeled apafant (10 μM) was then added and the reduction in specific binding was monitored over the next 180 min. *a* and *b*, Time course of [^{3}H]apafant dissociation from macrophages and the first-order transformation of these data, respectively. Data points represent the mean of duplicate determinations from a single experiment typical of three. See Materials and Methods for further details.

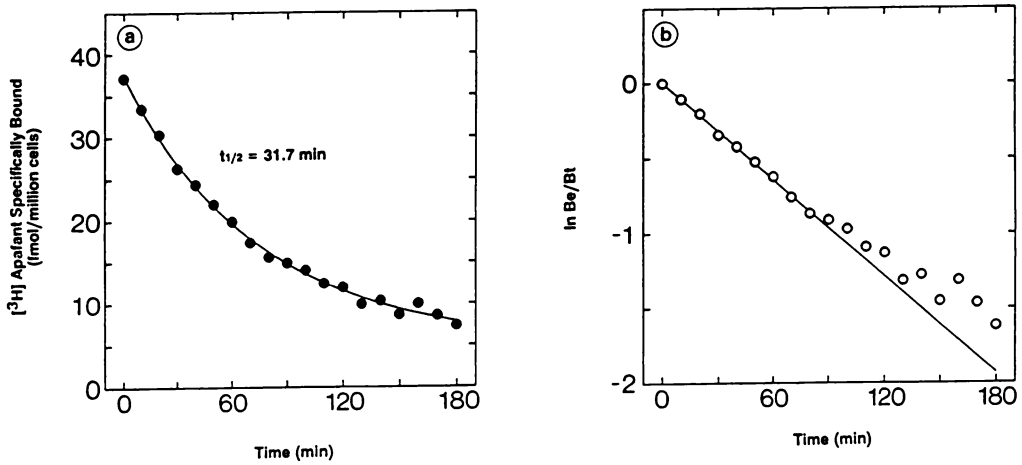

Fig. 4. Dissociation of [^{3}H]apafant from guinea pig intact peritoneal macrophages by unlabeled C_{18}-PAF (5 μM). *a* and *b*,Time course of [^{3}H] apafant dissociation from macrophages and first-order transformation of these data, respectively. Data points represent the mean of duplicate determinations from a single experiment typical of three. See legend to Fig. 2 and Materials and Methods for further details.

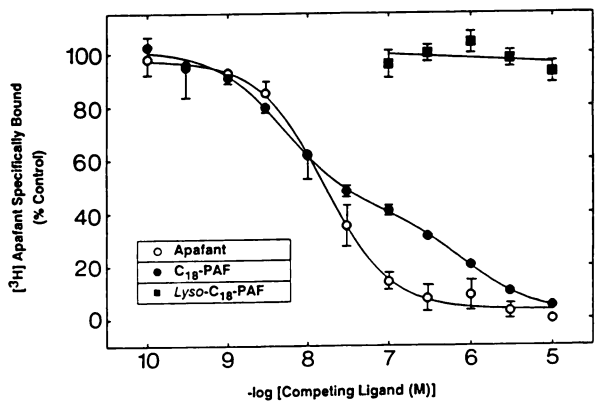

Fig. 5. Inhibition of specific [^{3}H]apafant binding to guinea pig intact macrophages by unlabeled apafant and C_{18}-PAF. Macrophages (~3 × 10^6/incubate) were incubated at 25° for 90 min in buffer C containing [^{3}H]apafant (10 nM) and unlabeled apafant (100 pM to 10 μM) (○), C_{18}-PAF (100 pM to 10 μM) (●), or *lyso*-C_{18}-PAF (100 nM to 10 μM) (■). Data points and error bars represent the mean ± standard error of three independent determinations performed in triplicate. See Materials and Methods for further details.

[^{3}H]apafant in intact cells (see above); steady state binding to each membrane preparation was reached within 50 min (Fig. 7). Similarly, the dissociation from membranes of [^{3}H]apafant (10 nM), bound at equilibrium, by a 1000-fold excess (10 μM) of unlabeled apafant was significantly faster ($t_{1/2}$ = 18.2 ± 0.9 min, n = 3; k_{off} = 0.032 ± 0.002 min^{-1}, n = 3) than that seen in intact cells but, nevertheless, was still slow (Fig. 8). From the k_{obs}, k_{off}, and concentration of [^{3}H]apafant used, the kinetically derived pK_d was calculated as 8.17.

Competition studies and the effect of guanine nucleotides. In view of the shallow competition curves obtained with C_{18}-PAF in intact cells (Table 1; Fig. 5), studies were performed in macrophage membranes to determine whether this was attributable to the presence of multiple conformational states of the apafant binding site. Consistent with the data obtained using intact cells, the C_{18}-PAF competition curves in membranes were shallow and were statistically better described by a two-site rather than a one-site model. It is notable that the affinity of C_{18}-PAF for the apafant binding site was higher in membranes than on intact cells irrespective of whether the data were analyzed assuming an interaction with one or two sites (Table 1).

Inclusion of the nonhydrolyzable guanine nucleotide analogue GTPγS (30 μM) in the binding buffer caused a ~30-fold decrease in the affinity of C_{18}-PAF for the apafant binding site (before GTPγS, pK_i = 8.48 ± 0.09; after GTPγS, pK_i = 7.56 ± 0.05, n = 6; $p < 0.05$) and an associated steepening (from 0.47 ± 0.03 to 0.7 ± 0.07, n = 6) of the C_{18}-PAF competition curve (Fig. 9). In contrast, GDPβS (30 μM) did not affect either of these parameters (data not shown).

Metabolism of C_{18}-PAF by Intact Macrophages

Incubation of guinea pig intact peritoneal macrophages at 25° with [^{3}H]C_{18}-PAF in the absence and presence of unlabeled

TABLE 1

Equilibrium inhibition constants (pK_i) and pseudo-Hill coefficients (n_H) of C_{18}-PAF for the antagonism of [^{3}H]apafant binding to guinea pig intact peritoneal macrophages and cell membranes

Intact peritoneal macrophages and cell membranes were incubated for 90 min at 25° with [^{3}H]apafant (10 nM) in the presence of increasing concentrations of unlabeled C_{18}-PAF (100 pM to 10 μM). Equilibrium inhibition constants were subsequently calculated according to the method of Cheng and Prussof (27), assuming that the data conformed to both one-site and two-site models, and pseudo-Hill coefficients were estimated from slopes of the logarithmically linearized data. See Materials and Methods for further details.

	One-site model		Two-site model			
	pK_i	n_H	pK_{i_H}	H	pK_{i_L}	L
				%		%
C_{18}-PAF, intact cells (n = 3)	7.87 ± 0.08	0.37 ± 0.02[a]	8.71 ± 0.11	60.1 ± 3.7	6.53 ± 0.09	39.9 ± 3.7
C_{18}-PAF, membranes (n = 3)	8.48 ± 0.09[b]	0.47 ± 0.03[a]	9.43 ± 0.33[b]	58.6 ± 3.3	7.74 ± 0.15[b]	41.4 ± 3.3

[a] $p < 0.01$, slope of competition curve significantly less than unity.
[b] $p < 0.05$, affinity of C_{18}-PAF significantly higher in membranes than in intact cells.

TABLE 2

Equilibrium inhibition constants (pK_i) and pseudo-Hill coefficients (n_H) of a range of structurally dissimilar PAF antagonists for the antagonism of [^{3}H]apafant binding to guinea pig intact peritoneal macrophages

Guinea pig intact peritoneal macrophages (2–4 × 10^6) were incubated for 90 min at 25° with [^{3}H]apafant (10 nM) in the presence of increasing concentrations (100 pM to 10 μM) of the PAF antagonists listed. The equilibrium inhibition constant for each PAF antagonist was subsequently calculated from its IC_{50} value by the method of Cheng and Prussof (27), and pseudo-Hill coefficients were estimated from slopes of the logarithmically linearized data. See Materials and Methods for further details.

Antagonist	n	pK_i	n_H
BN 50739	4	8.74 ± 0.04	−1.3 ± 0.1
UK 74,505	4	8.59 ± 0.04	−1.1 ± 0.1
STY 2108	4	8.38 ± 0.04	−1.1 ± 0.1
BN 50741	4	8.35 ± 0.08	−1.2 ± 0.2
Apafant	4	8.22 ± 0.09	−1.2 ± 0.2
Bepafant	4	8.00 ± 0.07	−1.1 ± 0.1

C_{18}-PAF (5 μM) resulted in a time-dependent reduction in the proportion of radiolabel that co-migrated with the [^{3}H]C_{18}-PAF standard (Table 3). This occurred in parallel with a time-dependent increase in the formation of radiolabeled products that had chromatographic identity with OAGPC and *lyso*-C_{18}-PAF (Table 3).

Fig. 9 shows that the relative proportion of lipid products produced by macrophages that co-migrated with the OAGPC and *lyso*-C_{18}-PAF standards depended upon the initial concentration of C_{18}-PAF in the incubation medium. Thus, in cells that were incubated with [^{3}H]C_{18}-PAF only (concentration, ~800 pM), the predominant metabolite resolved by TLC at all time points measured had chromatographic identity with authentic OAGPC; only a minor peak of radiolabel co-migrated with the *lyso*-C_{18}-PAF standard (Table 3). However, when the incubation buffer was supplemented with 5 μM unlabeled C_{18}-PAF, more tritium (~2-fold) was found in a product that co-migrated with the *lyso*-C_{18}-PAF rather than the OAGPC standard (Table 3).

It is important to note that the total radioactivity recovered from each lane of the TLC plate declined over the first hour of incubation, indicating that C_{18}-PAF was metabolized by macrophages into both lipophilic and water-soluble products (in addition to *lyso*-C_{18}-PAF and OAGPC) that were not resolved by TLC using the solvent system employed (Table 3).

Effect of Apafant on C_{18}-PAF-Induced Respiratory Burst

Under resting conditions there was a basal elaboration of $\cdot O_2^-$ from guinea pig macrophages that amounted to 3.1 ± 0.38 nmol/30 min/10^6 cells (n = 20). Challenge of cells with C_{18}-PAF (1 pM to 10 μM) resulted in a concentration-dependent generation of $\cdot O_2^-$ that was biphasic in nature (Fig. 10a). The pD_2 of C_{18}-PAF for the first phase of the response was 9.05 ± 0.12 (n = 5); an accurate estimate of the potency of C_{18}-PAF for eliciting the second phase of $\cdot O_2^-$ generation could not be determined due to the cytotoxic nature of C_{18}-PAF at concentrations above 30 μM (data not shown).

To confirm that C_{18}-PAF-induced respiratory burst activity in guinea pig peritoneal macrophages was mediated through agonism of specific cell surface PAF receptors, the ability of apafant (10 nM to 1 μM) to antagonize this response was

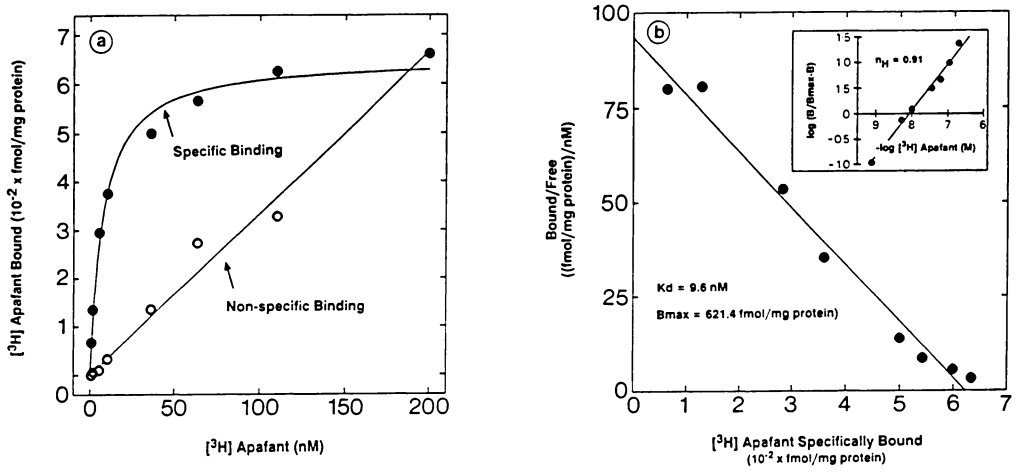

Fig. 6. Binding of [^{3}H]apafant to guinea pig peritoneal macrophage membranes. *a*, Representative saturation isotherm for [^{3}H]apafant. Binding was measured at 25° over a concentration range of 1–200 nM in buffer C containing ~200 μg of protein/incubate. Nonspecific binding was defined with 10 μM unlabeled apafant. *b*, Scatchard transformation of the data in *a* and the K_d and B_{max} values derived from this experiment. *b*, *inset*, Hill plot of the binding of [^{3}H]apafant to macrophage membranes. Results are typical of three determinations. See Materials and Methods for further details.

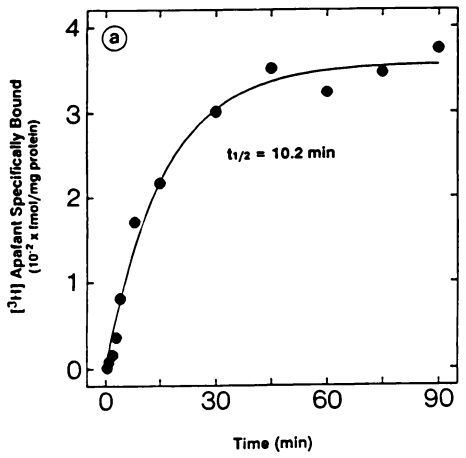

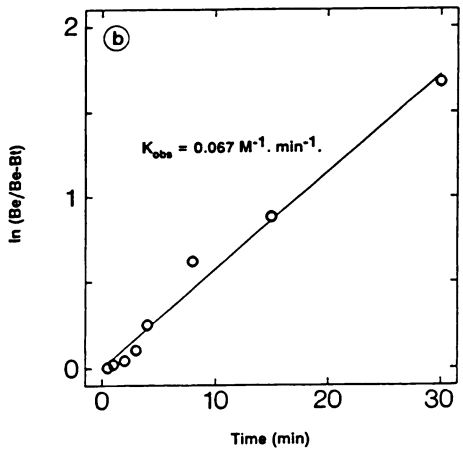

Fig. 7. Association of [3H]apafant with guinea pig peritoneal macrophage membranes. [3H]Apafant (10 nM) was incubated at 25° with membranes (~200 μg of protein/incubate) in buffer C for 1–90 min. Nonspecific binding was defined with 10 μM unlabeled apafant. *a* and *b*, Time course of [3H]apafant association with the membranes and the pseudo-first-order transformation of these data, respectively. Data points represent the mean of duplicate determinations from a single experiment typical of three. See Materials and Methods for further details.

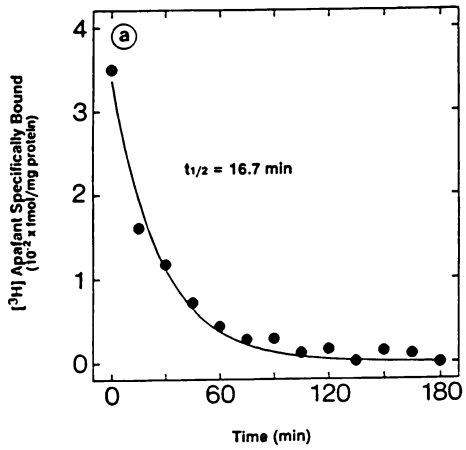

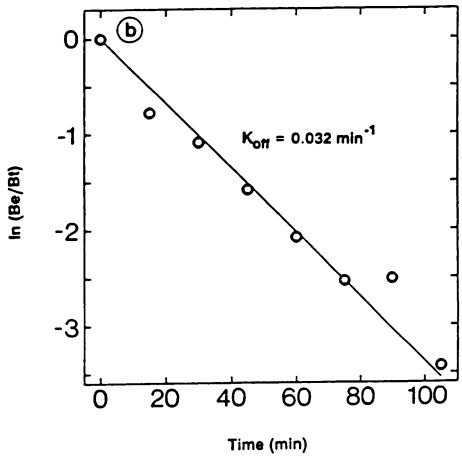

Fig. 8. Dissociation of [3H]apafant from guinea pig peritoneal macrophage membranes by unlabeled apafant (10 μM). *a* and *b*, Time course of [3H]apafant dissociation from macrophage membranes and first-order transformation of these data, respectively. Data points represent the mean of duplicate determinations from a single experiment typical of three. See legend to Fig. 6 and Materials and Methods for further details.

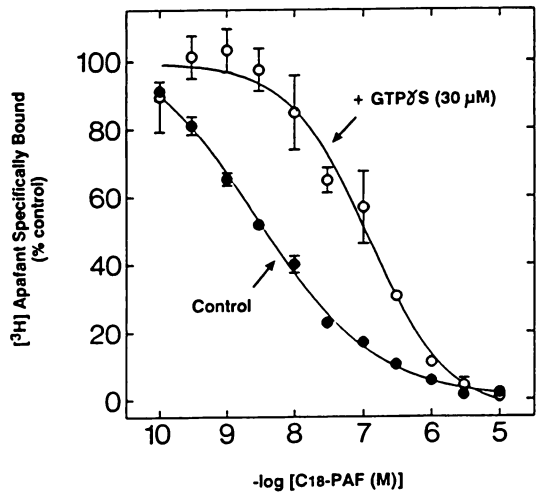

Fig. 9. Effect of GTPγS on the inhibition of [3H]apafant binding to guinea pig peritoneal macrophage membranes by C_{18}-PAF. Membranes (~200 μg/incubate) were incubated at 25° for 90 min in buffer C containing [3H] apafant (10 nM) and unlabeled C_{18}-PAF (100 pM to 10 μM) in the absence (●) and presence (○) of GTPγS (30 μM). Data points and error bars represent the mean ± standard error of six independent determinations performed in triplicate. See Materials and Methods for further details.

examined (Fig. 10a). In the absence of C_{18}-PAF, apafant did not significantly affect the spontaneaous generation of $\cdot O_2^-$, indicating that under the experimental conditions employed in this study there was no release of endogenously synthesized PAF at biologically active concentrations. Unexpectedly, and in contrast to the competitive behavior of this PAF antagonist observed in binding studies (see above), apafant antagonized the first phase of C_{18}-PAF-induced $\cdot O_2^-$ generation in an apparently noncompetitive manner (Fig. 10a): there was a progressive depression of the C_{18}-PAF concentration-response curves without a statistically significant increase in the EC_{50} of C_{18}-PAF except at the highest concentration of apafant studied (Fig. 10a).

The biphasic concentration-response curves elicited by C_{18}-PAF prompted studies to determine whether apafant could abolish the first and second components of this response. When C_{18}-PAF was used at a concentration (100 nM) that stimulated selectively the first phase of the respiratory burst, apafant inhibited this response completely, in a concentration-dependent fashion ($pIC_{50} = 6.80 \pm 0.14$, $n = 4$); inhibition was maximal at 1 μM apafant (Fig. 10b). In contrast, apafant was ~40-fold less potent ($pIC_{50} = 5.23 \pm 0.44$, $n = 5$) and produced only a partial inhibition (59.8 ± 4.2% at 100 μM apafant, $n = 5$) of $\cdot O_2^-$ generation when C_{18}-PAF was used at a higher concentration (10 μM). Indeed, the second phase of C_{18}-PAF-induced respiratory burst was essentially resistant to apafant (Fig. 10b).

Discussion

On guinea pig intact peritoneal macrophages, [3H]apafant labeled a homogeneous population of noninteracting binding sites. The observation that [3H]apafant binding was concentration dependent, saturable, reversible, of high affinity, and an-

TABLE 3

Quantitative distribution of tritium in lipid products after incubation of guinea pig intact peritoneal macrophages with [^{3}H]C_{18}-PAF

Cells were incubated at 25° with [^{3}H]C_{18}-PAF (800 pM) or [^{3}H] C_{18}-PAF (800 pM) supplemented with unlabeled C_{18}-PAF (5 μM), for 1, 2, and 3 hr, and the lipids were extracted and subjected to TLC as described in Materials and Methods. Results are given as absolute dpm in radiolabeled lipid products formed that had chromatographic identity with authentic C_{18}-PAF, *lyso*-C_{18}-PAF, and OAGPC standards. Values in parentheses represent the percentage of radiolabeled lipid products formed with respect to the [^{3}H]C_{18}-PAF standard (taken as 100%). Values represent the mean ± standard error of three independent observations from different cell preparations.

	Radioactivity			
	Total[a]	[^{3}H]C_{18}-PAF	*lyso*-C_{18}-PAF	OAGPC
	dpm			
[^{3}H]C_{18}-PAF (800 pM)				
Std[b]	40,168 ± 1,510	37,547 ± 1,340 (100)[b]		
1 hr	35,073 ± 2,071[c]	25,674 ± 2,113 (68.4)	2,246 ± 308 (6)	6,206 ± 1,382 (16.5)
2 hr	34,166 ± 2,480[c]	19,865 ± 2,324 (52.9)	2,722 ± 418 (7.2)	10,004 ± 1,430 (26.6)
3 hr	37,791 ± 2,713	18,915 ± 2,606 (50.3)	3,338 ± 417 (8.9)	13,804 ± 2,278 (36.7)
[^{3}H]C_{18}-PAF (800 pM) + C_{18}-PAF (5 μM)				
Std[b]	44,036 ± 1,743	42,035 ± 1,646 (100)[b]		
1 hr	32,699 ± 758[c]	30,914 ± 1,263 (73.5)	2,044 ± 341 (4.9)	1,345 ± 272 (3.2)
2 hr	34,783 ± 293[c]	26,022 ± 1,581 (61.9)	3,794 ± 494 (9)	2,702 ± 568 (6.4)
3 hr	35,311 ± 1,292[c]	23,977 ± 1,277 (57)	5,263 ± 1,131 (12.5)	3,586 ± 666 (8.5)

[a] Total dpm recovered from each lane of the TLC plate.
[b] Std, [^{3}H]C_{18}-PAF standard, which amounted to >93% of the "total" radioactivity recovered at time = 0 hr.
[c] $p < 0.05$, significant reduction in radioactivity recovered from each lane of the TLC plate.

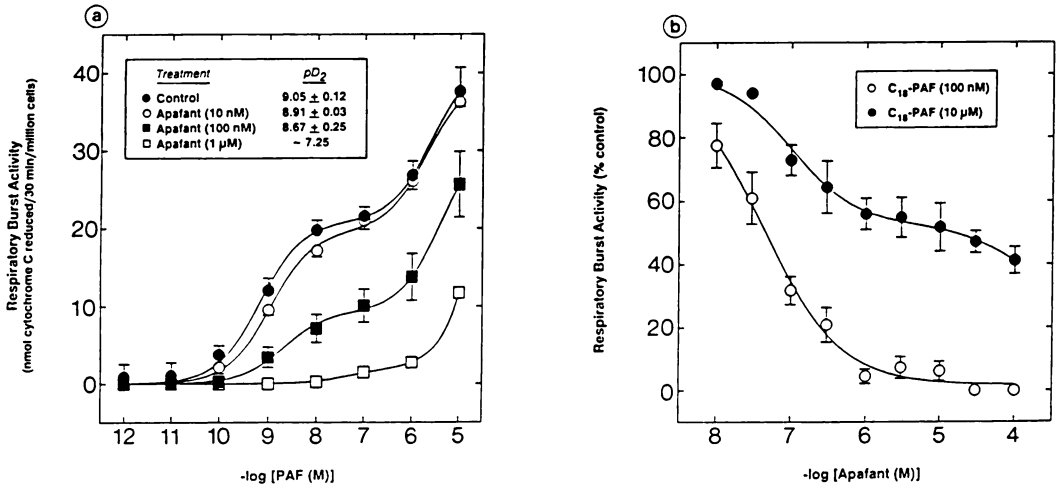

Fig. 10. Stimulation by C_{18}-PAF of $\cdot O_2^-$ generation from guinea pig peritoneal macrophages at 37° and its antagonism by apafant. *a*, Concentration-response curves for C_{18}-PAF (1 pM to 10 μM) effects on respiratory burst activity in the absence (●) and in the presence of 10 nM (○), 100 nM (■), and 1 μM (□) apafant. *b*, Inhibitory effect of apafant (10 nM to 100 μM) on respiratory burst activity induced by 100 nM (○) and 10 μM (●) C_{18}-PAF. Data points represent the mean ± standard error of *n* independent determinations performed in duplicate. Error bars are not shown when they fall within the size of the symbol. See Materials and Methods for further details.

tagonized by a range of structurally dissimilar PAF antagonists and by the natural ligand C_{18}-PAF (but not by *lyso*-C_{18}-PAF, the functionally inactive precursor and metabolite of C_{18}-PAF) suggests that these binding sites represent *bona fide* PAF receptors.

[^{3}H]Apafant bound to intact macrophages with an equilibrium pK_d of 8.23. Although this value is in good agreement with its affinity for the PAF receptors on human platelets (pK_d = 8.21) (30) it differs from that reported for apafant on human neutrophils (pK_d = 7.72) (31), guinea pig peritoneal eosinophils (pK_d = 7.79) (32), human peripheral blood eosinophils (pK_d = 7.73) (32), guinea pig lung membranes [pK_d = 7.77 (33) or pK_d = 7.39 (16)], and human lung membranes (pK_d = 7.65) (33). Although this discrepancy may be due to PAF receptor heterogeneity between different cell types (see, for example, Refs. 9, 34, and 35), it cannot, at the present time, be claimed reasonably that such a small difference in affinity indicates distinct PAF receptor classes.

Consistent with radioligand binding data published from other laboratories, apafant interacted with macrophages in an apparently competitive manner, with pseudo-Hill coefficients derived from both saturation and competition studies not significantly different from unity, thus indicating that apafant did not interact cooperatively with these PAF receptors.

A perplexing finding that emerged from these studies was the 40–50-fold discrepancy between the affinity of apafant calculated from our binding studies (pK_i/pK_d, ~8.25) and that reported by Stewart and Dusting (9) for the antagonism of PAF-induced prostacyclin release (pA_2 = 6.62). One possible explanation for these results is that PAF-induced arachidonic acid metabolism is not mediated by the same population of PAF receptors labeled by [^{3}H]apafant in binding experiments. If this is true, then the question that must be addressed is as follows: do macrophages express PAF receptors for which apafant has low affinity? Our binding data do not support this hypothesis. Even though the highest concentration of [^{3}H] apafant (200 nM) used in saturation studies was essentially equal to the affinity of apafant calculated from functional experiments (antilog −6.62 = 240 nM), the binding of this PAF antagonist to macrophages conformed to a simple hyperbola from which a linear Scatchard plot was derived. Apafant thus apparently labeled a homogeneous population of sites. It is

important to include a caveat here because apafant may, indeed, bind to a population of PAF receptors on macrophages with low affinity (possibly mediating prostacyclin release) but their number may be so small relative to the total apafant-sensitive PAF receptor density that they were not detected. It is noteworthy that more recently Stewart (36) has contradicted the original report of Stewart and Dusting (9), i.e., that apafant is a competitive antagonist at the macrophage PAF receptor (see above), and now suggests a noncompetitive interaction (see below). If the latter proposal is true, and evidence published recently is consistent with this (see Refs. 6 and 37), then the pA_2 calculated by Stewart and Dusting (9) from functional studies is clearly an unreliable estimate of the affinity of apafant for this PAF receptor.

Another striking observation was that the maximum number of binding sites identified by [^{3}H]apafant on guinea pig peritoneal macrophages (~33,600/cell) was approximately 4-fold lower than that reported by Floch *et al.* (6), who used [^{3}H]PAF as radioligand. This inconsistency, however, is seemingly not peculiar to macrophages. Indeed, marked variations between the B_{max} values for [^{3}H]apafant and [^{3}H]PAF have been reported in several other types of cells of myeloid origin. For example, Dent *et al.* (31) calculated that there are ~40,000 binding sites for [^{3}H]apafant on human neutrophils, whereas Valone and Goetzl (38) reported that [^{3}H]PAF labels 5,200,000 sites on this cell type. Although the reason for these discrepancies is not clear, at least two possibilities should be considered. The first is that [^{3}H]apafant has high affinity for only a minor proportion (25% in the macrophage) of the cell surface receptors labeled by [^{3}H]PAF. The other, and perhaps more likely, explanation is that [^{3}H]PAF binds specifically to intracellular and extracellular sites in addition to the PAF receptor. Some support for this contention is provided by Floch *et al.* (6), who reported that [^{3}H]PAF binds irreversibly to macrophages. It is clear, therefore, that if this latter hypothesis is correct then binding data obtained with [^{3}H]PAF should be interpreted cautiously. This also highlights the advantages of using metabolically stable, hydrophilic antagonists in binding experiments.

To characterize further the PAF receptor on macrophages the ability of a number of novel, structurally dissimilar, PAF antagonists to compete with [^{3}H]apafant was examined. All of the antagonists inhibited apafant binding with pseudo-Hill coefficients not significantly different from unity and with a rank order of potency in good agreement with their ability to inhibit PAF-induced functional responses (39, 40). Our finding that BN 50739 had the highest affinity for the apafant-sensitive PAF receptors on macrophages supports the recent assertion (41, 42) that BN 50739 is one of the most potent PAF antagonists currently availaible.

In agreement with the binding data obtained in intact macrophages (see above), [^{3}H]apafant bound also, in a competitive manner, to a homogeneous population of noninteracting sites on macrophage membranes. A number of quantitative differences, however, were observed. In particular, the rate at which [^{3}H]apafant associated with and dissociated from macrophages was significantly faster in membrane preparations. Furthermore, the affinity of C_{18}-PAF for the apafant binding site was between 0.5 and 1 log unit higher in membranes irrespective of whether the data were constrained to a one-site or two-site model. The reasons for these differences are not clear but may reflect in part the loss, upon cell lysis, of certain cytosolic factors that regulate the conformation and function of the PAF receptor.

C_{18}-PAF also competed with [^{3}H]apafant for the macrophage PAF receptors on intact cells and in macrophage membranes but, in contrast to the PAF antagonists studied, yielded shallow inhibition curves that were statistically better described by a two-site rather than a one-site model. Such binding data are taken to indicate either receptor heterogeneity or the presence of a single population of receptors that exist in at least two interconvertible conformational states, for which the agonist has high and low affinity. Given that there is little convincing evidence for multiple PAF receptors within species, it was reasoned that the shallow inhibition curves obtained with C_{18}-PAF were due to different conformational states of the same PAF receptor. Indeed, the finding that GTPγS, but not GDPβS, reduced the affinity of C_{18}-PAF >30-fold and increased markedly the slope of the competition curve is consistent with this hypothesis.

It is well established that PAF is a potent stimulant of the respiratory burst oxidase in macrophages (e.g., Refs. 4–6 and 11). Although the studies reported herein confirm this, they suggest also that this effect of PAF is complex. Evidence to support this is twofold; 1) the concentration-response curves that described $\cdot O_2^-$ generation were biphasic and 2) the second component of the respiratory burst was insensitive to apafant. At least two theories can be advanced to explain these results. The first is that macrophages express two populations of PAF receptors, for which C_{18}-PAF has different affinities and only one of which is recognized by apafant. Some data to support this contention can be derived from the finding that apafant is >100-fold less potent as an antagonist of $\cdot O_2^-$ generation in guinea pig peritoneal eosinophils than it is as an antagonist of degranulation (43). The other consideration is that the apafant-sensitive component of PAF-induced $\cdot O_2^-$ generation is mediated by a mechanism that does not involve agonism of PAF receptors. Although the lipophilicity of PAF prompts speculation that it may act as an intracellular messenger, it remains to be established whether the respiratory burst oxidase can be activated by PAF in a receptor-independent manner.

Given the competitive nature of apafant in binding studies, it was surprising that functionally (inhibition of respiratory burst) this antagonist behaved in an apparently noncompetitive manner. This unexpected behavior of apafant has been reported previously for PAF-induced thromboxane B_2 release from guinea pig peritoneal eosinophils (37), PAF-induced chemiluminescence in human granulocytes (6), and PAF-induced prostacyclin release and respiratory burst activity in guinea pig peritoneal macrophages (6, 36). Until now no theory has been advanced to explain these unexpected results. Our kinetic data, however, suggest that the apparently noncompetitive behavior of apafant observed in functional studies may relate to the very slow rate ($t_{½}$, ~32 min) at which the antagonist is displaced from the PAF receptor by C_{18}-PAF. Therefore, we suggest that, when the effects of apafant are examined on PAF-induced functional responses that are characteristically rapid and transient (e.g., $\cdot O_2^-$ generation in macrophages), the slow off-rate of apafant effectively reduces the number of available PAF receptors that C_{18}-PAF can occupy. As such, apafant behaves as if it were a noncompetitive antagonist.

An observation that we considered necessary to investigate

further was the apparently complex kinetics that described the displacement of [^{3}H]apafant from intact macrophages by unlabeled C_{18}-PAF. Because this was not seen when unlabeled apafant was used as displacing ligand, it was reasoned that significant enzymatic metabolism of C_{18}-PAF occurring at late time points may be the cause of this anomaly. Guinea pig peritoneal macrophages readily metabolized C_{18}-PAF in a time-dependent manner at 25°, yielding *lyso*-C_{18}-PAF and a product that had chromatographic identity with OAGPC. This profile of metabolites agrees with that reported by Valone (20) for murine P388D$_1$ macrophages and is consistent with the fact that these cells synthesize and release acetylhydrolases (44, 45) and express an effective polyenoate transacylation capacity (46, 47). Because the R_F values of alkylacylglycerophosphocholines are essentially the same irrespective of the acyl group at the *sn*-2-position, under the experimental conditions used in these studies, it was not possible to identify the fatty acid substituent of the major transacylation products. However, in many different cells including macrophages (46) *lyso*-PAF is acylated by an enzyme that shows selectivity for arachidonate (3).

In conclusion, the results of this study demonstrate that guinea pig peritoneal macrophages express *bona fide* PAF receptors for which [^{3}H]apafant and a number of other structurally dissimilar PAF antagonists have high affinity. These data are also consistent with the hypothesis that apafant-sensitive PAF receptors on these cells are coupled to guanine nucleotide-binding proteins and can exist in at least two interconvertible and guanine nucleotide-regulated conformational states. Finally, the very slow rate at which apafant dissociates from the macrophage PAF receptors may explain why apafant behaves as a noncompetitive PAF antagonist in these cells.

Acknowledgments

The authors thank Dr. P. Braquet, Institute Henri Beaufour (Paris, France), Dr. V. Alabaster, Pfizer Central Research (Sandwich, Kent, UK), and Dr. H. Heuer, Boehringer Ingelheim KG (Ingelheim am Rhein, Germany) for the gifts of drugs.

References

1. Pinckard, R. N., E. M. Jackson, C. Hoppens, S. T. Weintraub, J. C. Ludwig, L. M. McManus, and G. E. Mott. Molecular heterogeneity of platelet activating factor produced by stimulated human polymorphonuclear leukocytes. *Biochem. Biophys. Res. Commun.* **122**:325–332 (1984).
2. Mallet, A. J., F. M. Cunningham, and F. Daniel. Rapid isocratic high performance liquid chromatographic purification of platelet activating factor (PAF) and *lyso*-PAF from human skin. *J. Chromatogr.* **309**:160–164 (1984).
3. Snyder, F. Platelet activating factor and related acetylated lipids as potent biologically active cellular mediators. *Am. J. Physiol.* **259**:C697-C708 (1990).
4. Hartung, H.-P., M. J. Parnham, J. Winkelmann, W. Engelberger, and U. Hadding. Platelet activating factor (PAF) induces the oxidative burst in macrophages. *Int. J. Immunopharmacol.* **5**:115–121 (1983).
5. Huang, S. J., P. N. Monk, C. P. Downes, and A. D. Whetton. Platelet activating factor-induced hydrolysis of phosphatidylinositol 4,5-bisphosphate stimulates the production of reactive oxygen intermediates in macrophages. *Biochem. J.* **249**:839–845 (1988).
6. Floch, A., L. Tahraoui, and I. Cavero. The platelet activating receptor antagonist, RP 59227, blocks platelet activating factor receptors mediating liberation of reactive oxygen species in guinea pig macrophages and human polymorphonuclear leukocytes. *J. Pharmacol. Exp. Ther.* **258**:567–575 (1991).
7. Scharberg, T., H. Haller, and H. Lode. Evidence for a platelet activating factor receptor on human alveolar macrophages. *Biochem. Biophys. Res. Commun.* **177**:704–710 (1991).
8. Hartung, H.-P. Acetyl glyceryl ether phosphorycholine (platelet activating factor) mediates heightened metabolic activity in macrophages: studies on PGE, TXB_2 and O_2^- production, spreading, and the influence of calmodulin inhibitor W-7. *FEBS Lett.* **160**:209–212 (1983).
9. Stewart, A. G., and G. J. Dusting. Characterization of receptors for platelet activating factor on platelets, polymorphonuclear leukocytes and macrophages. *Br. J. Pharmacol.* **94**:1225–1233 (1988).
10. Masliah, J., M. Bachelet, O. Colard, G. Bereziat, and B. B. Vargaftig. Mobilization of arachidonic acid from diacyl and ether-linked phospholipids in FMLP stimulated macrophages. *Biochem. Pharmacol.* **37**:547–550 (1988).
11. Kadiri, C., J. Masliah, M. Bachelet, B. B. Vargaftig, and G. Bereziat. Phospholipase A_2-mediated release of arachidonic acid in stimulated guinea pig alveolar macrophages: interaction with lipid mediators and cyclic AMP. *J. Cell. Biochem.* **40**:157–164 (1989).
12. Prpic, V., R. J. Uhling, J. E. Weiel, L. Jakoi, G. Gawadi, B. Herman, and D. O. Adams. Biochemical and functional responses stimulated by platelet activating factor in murine peritoneal macrophages. *J. Cell. Biol.* **107**:363–372 (1988).
13. Hayashi, H., I. Kudo, H. Inoue, H. Nomura, and S. Nojima. Macrophage activation by PAF incorporated into dipalmitoylphosphatidylcholine-cholesterol liposomes. *J. Biochem. (Toyko)* **97**:1255–1258 (1985).
14. Conrad, G. W., and T. J. Rink. Platelet activating factor raises intracellular calcium ion concentration in macrophages. *J. Cell. Biol.* **103**:439–450 (1986).
15. Dent, G., D. Ukena, and P. J. Barnes. PAF receptors, in *Platelet Activating Factor and Human Disease* (P. J. Barnes, C. P. Page, and P. M. Henson, eds.). Blackwell Scientific, Oxford, 58–81 (1989).
16. Gomez, J., J. W. Bloom, H. I. Yamamura, and M. Halonen. Characterization of receptors for platelet-activating factor in guinea pig lung membranes. *Am. J. Respir. Cell. Mol. Biol.* **3**:259–264 (1990).
17. Honda, Z., M. Nakamura, I. Miki, M. Minami, T. Watanabe, Y. Seyama, H. Okado, H. Toh, K. Ito, T. Miyamoto, and T. Shimizu. Cloning by functional expression of platelet activating factor receptor from guinea pig lung. *Nature (Lond.)* **349**:343–346 (1991).
18. Nakamura, M., Z. Honda, T. Izumi, C. Sakanaka, H. Mutoh, M. Minami, H. Bito, Y. Seyama, T. Matsumoto, M. Noma, and T. Shizumi. Molecular cloning and expression of platelet activating factor receptor from human leukocytes. *J. Biol. Chem.* **266**:20400–20405 (1991).
19. Hayashi, H., I. Kudo, K. Inoue, K. Onozaki, S. Tsushima, H. Nomura, and S. Nojima. Activation of guinea pig peritoneal macrophages by platelet activating factor (PAF) and its analogues. *J. Biochem. (Tokyo)* **97**:1737–1745 (1985).
20. Valone, F. H. Identification of platelet activating receptors in P388D$_1$ murine macrophages. *J. Immunol.* **140**:2389–2394 (1988).
21. Casals-Stenzel, J., G. Muacevic, and K. H. Weber. Pharmacological actions of WEB 2086, a new specific antagonist of platelet activating factor. *J. Pharmacol. Exp. Ther.* **241**:974–981 (1987).
22. Hwang, S.-B., M.-H. Lam, and A. H.-M. Hsu. Characterization of platelet-activating factor (PAF) receptor by specific binding of [^{3}H]L-659,989, a PAF receptor antagonist, to rabbit platelet-membranes: possible multple conformational states of a single type of PAF receptors. *Mol. Pharmacol.* **35**:48–58 (1989).
23. Ring, P. C., P. M. Seldon, R. S. Perkins, G. Dent, P. J. Barnes, and M. A. Giembycz. Identification and partial characterisation of a receptor for platelet activating factor on guinea pig peritoneal macrophages. *Br. J. Pharmacol.* **104**:85P (1991).
24. Ring, P. C., P. J. Barnes, and M. A. Giembycz. Effect of guanine nucleotides on the binding of platelet activating factor (PAF) to guinea pig peritoneal macrophage membranes. *Respir. Med.* **86**:79 (1992).
25. Gartner, I. Separation of human eosinophils in density gradients of polyvinylpyrrolidone-coated silica gel (Percoll). *Immunology.* **40**:133–136 (1980).
26. Lowry, O. H., N. J. Rosebrough, A. L. Farr, and R. J. Randall. Protein measurement with the Folin phenol reagent. *J. Biol. Chem.* **193**:265–275 (1951).
27. Cheng, Y.C., and W. H. Prusff. Relationship between the inhibition constant (K_i) and the concentration of inhibitor which causes 50 percent inhibition (I_{50}) of an enzymatic reaction. *Biochem. Pharmacol.* **22**:3099–3108 (1973).
28. Johnson, R. B., B. B. Keele, H. P. Misra, J. E. Leymeyer, L. S. Webb, R. L. Baehner, and K. V. Rajogopalan. The role of superoxide anion generation in phagocytic bactericidal activity: studies with normal and chronic granulomatous disease leukocytes. *J. Clin. Invest.* **55**:1357–1372 (1975).
29. Pick, E., and D. Mizel. Rapid microassays for the measurement of superoxide and hydrogen peroxide production by macrophages in culture using an automated enzyme immunoassay reader. *J. Immunol. Methods* **46**:211–216 (1981).
30. Ukena, D., G. Dent, F. W. Birke, C. Robaut, G. W. Sybrecht, and P. J. Barnes. Radioligand binding of antagonists of platelet activating factor to intact human platelets. *FEBS Lett.* **228**:285–289 (1988).
31. Dent, G., D. Ukena, P. Chanez, G. W. Sybrecht, and P. J. Barnes. Characterization of PAF receptors on human neutrophils using the specific antagonist, WEB 2086: correlation between binding and function. *FEBS Lett.* **244**:365–368 (1989).
32. Ukena, D., C. Kroegel, T. Yukawa, G. W. Sybrecht, and P. J. Barnes. PAF receptors on eosinophils: identification with a novel ligand, [^{3}H]WEB 2086. *Biochem. Pharmacol.* **38**:1702–1705 (1989).
33. Dent, G., D. Ukena, G. W. Sybrecht, and P.J. Barnes. [^{3}H]WEB 2086 labels platelet activating factor receptors in guinea pig and human lung. *Eur. J. Pharmacol.* **169**:313–316 (1989).
34. Lambrecht, G., and M. J. Parnham. Kadsurenone distinguishes between different platelet activating receptor subtypes on macrophages and polymorphonuclear leukocytes. *Br. J. Pharmacol.* **87**:287–289 (1986).
35. Hwang, S.-B. Identification of a second putative receptor of platelat activating factor from polymorphonuclear leukocytes. *J. Biol. Chem.* **263**:3225–3233 (1988).

36. Stewart, A. G. Heterogeneity of platelet activating factor receptors on platelets and macrophages. *J. Lipid Mediators* **2**:204 (1990).
37. Giembycz, M. A., C. Kroegel, and P. J. Barnes. Platelet activating factor stimulates cyclo-oxygenase activity in guinea pig eosinophils: concerted biosynthesis of thromboxane A_2 and E-series prostaglandins. *J. Immunol.* **144**:3489–3497 (1990).
38. Valone, F. H., and E. J. Goetzl. Specific binding by human polymorphonuclear leukocytes of the immunological mediator 1-*O*-hexadecyl/octadecyl-2-acetyl-*sn*-glycero-3-phosphorylcholine. *Immunology* **48**:141–149 (1983).
39. Heuer, H. O., J. Casals-Stenzel, G. Muacevic, and K.-H. Weber. Pharmacologic activity of bepafant (WEB 2170), a new and selective hetrazepine antagonist of platelet activating factor. *J. Pharmacol. Exp. Ther.* **255**:962–967 (1990).
40. Yue, T.-L., M. M. Gleason, J.-L. Gu, P. G. Lysko, J. Hallenbeck, and G. Feuerstein. Platelet activating factor (PAF) receptor-mediated calcium mobilization and phosphoinositide turnover in neurohybrid NG108–15 cells: studies with BN 50739, a new PAF antagonist. *J. Pharmacol. Exp. Ther.* **257**:374–381 (1991).
41. Yue, T.-L., M. Farhat, R. Rabinovici, P. Y. Perera, S. N. Vogel, and G. Feuerstein. Protective effect of BN 50739, a new platelet activating factor antagonist, in endotoxin-treated rabbits. *J. Pharmacol. Exp. Ther.* **254**:976–981 (1990).
42. Yue, T.-L., R. Rabinovici, M. Farhat, and G. Feuerstein. Pharmacological profile of BN 50739, a new PAF antagonist *in vitro* and *in vivo*. *Prostaglandins* **39**:469–480 (1990).
43. Kroegel, C., T. Yukawa, J. Westwick, and P. J. Barnes. Evidence for two platelet activating receptors on eosinophils: dissociation between PAF-induced intracellular calcium mobilization, degranulation, and superoxide anion generationin eosinophils. *Biochem. Biophys. Res. Commun.* **162**:511–521 (1989).
44. Elstad, M. R., D. M. Stafforini, T. M. McIntyre, S. M. Prescott, and G. A. Zimmerman. Platelet activating factor acetylhydrolase increases during macrophage differentiation: a novel mechanism that regulates accumulation of platelet activating factor. *J. Biol. Chem.* **264**:8467–8470 (1989).
45. Stafforini, D. M., M. R. Elstad, T. M. McIntyre, G. A. Zimmerman, and S. M. Prescott. Human macrophages secrete platelet activating factor acetylhydrolase. *J. Biol. Chem.* **265**:9682–9687 (1990).
46. Robinson, M., M. L. Blank, and F. Snyder. Acylation of lysophospholipids by rabbit alveolar macrophages: specificities of CoA-dependent and CoA-independent reactions. *J. Biol. Chem.* **260**:7889–7895 (1985).
47. Sugiura, T., and K. Waku. CoA-independent transfer of arachidonic acid from 1,2-diacyl-*sn*-glycero-3-phosphocholine to 1-*O*-alkyl-*sn*-glycero-3-phosphocholine (*lyso*-platelet activating factor) by macrophage microsomes. *Biochem. Biophys. Res. Commun.* **127**:384–390 (1985).

Send reprint requests to: Mark A. Giembycz, Ph.D., Department of Thoracic Medicine, Royal Brompton National Heart and Lung Institute, Dovehouse Street, London SW3 6LY, UK.